Hindawi Publishing Corporation
ISRN Chemical Engineering
Volume 2013, Article ID 930484, 11 pages
http://dx.doi.org/10.1155/2013/930484

Research Article

Prediction the Vapor-Liquid Equilibria of CO_2-Containing Binary Refrigerant Mixtures Using Artificial Neural Networks

Ahmad Azari,[1] Saeid Atashrouz,[2] and Hamed Mirshekar[2]

[1] *Chemical Engineering Department, Gas and Petrochemical Engineering Faculty, Persian Gulf University, Bushehr 7516913817, Iran*
[2] *Department of Petrochemical Engineering, Amirkabir University of Technology (Tehran Polytechnic), Mahshahr Campus, P.O. Box 415, Mahshahr, Iran*

Correspondence should be addressed to Saeid Atashrouz; s.atashrouz@gmail.com

Received 9 May 2013; Accepted 18 July 2013

Academic Editors: J. A. A. González, K. Okumura, and J. E. Ten Elshof

Artificial neural network (ANN) technique has been applied for estimation of vapor-liquid equilibria (VLE) for eight binary refrigerant systems. The refrigerants include difluoromethane (R32), propane (R290), 1,1-difluoroethane (R152a), hexafluoroethane (R116), decafluorobutane (R610), 2,2-dichloro-1,1,1-trifluoroethane (R123), 1-chloro-1,2,2,2-tetrafluoroethane (R124), and 1,1,1,2-tetrafluoroethane (R134a). The related experimental data of open literature have been used to construct the model. Furthermore, some new experimental data (not applied in ANN training) have been used to examine the reliability of the model. The results confirm that there is a reasonable conformity between the predicted values and the experimental data. Additionally, the ability of the ANN model is examined by comparison with the conventional thermodynamic models. Moreover, the presented model is capable of predicting the azeotropic condition.

1. Introduction

For nearly 60 years, chlorofluorocarbons (CFCs) have been widely used as solvents, foam blowing agents, aerosols, and especially refrigerants due to their stability, nontoxicity, nonflammability, good thermodynamic properties, and so on. However, they also have a harmful effect on the earth's protective ozone layer. So, they have been regulated internationally by Montreal Protocol since 1987. Much effort has been made to find the suitable replacement for CFCs. Initial CFC alternatives included some hydrochlorofluorocarbons (HCFCs), but they will be also phased out internationally because their ozone depletion potentials (ODPs) and global warming potentials (GWPs) are significant though less than those of CFCs. Hydrofluorocarbons (HFCs) synthetic refrigerants which have zero ODPs were proposed as promising replacements for CFCs and HCFCs [1]. The deadline for HCFCs which have low ozone depletion potential is 2030. Also there is no report for another type of refrigerants such as light hydrocarbons or perfluorocarbons as harmful refrigerants. In order to develop new refrigerants for replacement with harmful refrigerants, the mixtures of carbon dioxide and clean refrigerants have been studied in the number of researches [2–8] that was reviewed in the present study.

R134a is an environmentally acceptable refrigerant, which has replaced the ozone-depleting CFC-12 (dichlorodifluoromethane) in a wide range of applications especially in automotive air conditioning and domestic refrigeration. Another natural refrigerant, carbon dioxide (R744), has received new worldwide interest as a working fluid in automotive air conditioning. To expand the range of possible replacement fluid with desired properties, phase behavior of R134a-R744 should be studied. This clean mixture can be formulated so as to obtain a similar vapor pressure to that of the original refrigerant, to suppress flammability or toxicity of one of the components that otherwise has excellent thermophysical properties [5].

R152a is used for refrigeration and as an aerosol propellant. It is most commonly found in electronic cleaning products and many consumer aerosol products that must meet stringent volatile organic compounds (VOC) requirements [8]. Such as the mixture of R134a-R744, prediction of vapor-liquid equilibria (VLE) for the mixture of R152a-R744 is

necessary for the development of new refrigerant mixtures with minimal environmental impact.

R116 and R744 (CO_2) are two very interesting fluids for industry. Their common peculiarity is their low critical temperatures. The critical temperature of CO_2 is 304.20 K, while that of R116 is 293.04 K. Moreover, this system presents azeotropic behavior, indicating strong interaction between the two species, in particular a strong repulsive interaction. Azeotropic and even quasiazeotropic behaviors are of utmost interest not only to refrigeration industry but also to all industries involved in supercritical fluid extraction. Utilization of fluids with low critical points that are also safe for the environment is generally highly preferred. An azeotropic mixture of R116 and R744 could be very interesting for industry of refrigeration as the azeotrope position is at high R744 composition [6]. So it is useful to study the VLE of this type of mixtures.

The mixture of CO_2-R610 (perfluorocarbons) is another type of refrigerants. In addition to the role of a refrigerant, this mixture has another application. This application is ability of perfluorocarbons in dissolving refinery gases such as CO_2, and it is necessary to prediction of phase behavior for this mixture [7].

R123 and R124 are two new clean fire extinguishing agents in comparison to other agents. For the new total flooding clean agents that were being developed to replace certain Halon fire extinguishing agents, the discharge time required to achieve 95% of the minimum design concentration shall not exceed 10 s, and the expellant gas is needed for its lack of vapor pressure. Generally, nitrogen is used as an expellant gas because it does not need to be liquefied at high pressure, but CO_2 has some merits to nitrogen such as price, storage area, and supplementary extinguishing effect. When CO_2 is used as an expellant gas, the knowledge of the phase behavior of the mixtures, CO_2 and fire extinguishing agents, is essential to design fire extinguishing processes and equipments. Moreover, phase equilibrium data are needed to calculate the friction loss along with the working plans (from the storage tank to the discharge orifice) [2].

Hydrocarbons like propane, butane, and isobutane have excellent thermophysical properties and are compatible with materials normally used in refrigeration plants such as copper. However, the flammability of hydrocarbons limits their application to specific systems. Carbon dioxide has advantages of being nontoxic, inflammable, and high in volumetric capacity of refrigeration. However, the refrigeration system using carbon dioxide is operated under a very high pressure. Hydrocarbons would reduce the problems occurring due to high pressure of carbon dioxide while carbon dioxide would reduce the flammability of hydrocarbons. The mixtures of carbon dioxide and propane (R290) are proposed as promising alternative refrigerants. The VLE data are essential to evaluate the performance of the refrigeration or the heat pump cycles using these refrigerant mixtures and to determine the optimum composition for the best performance [3].

Information about the phase behavior of refrigerant mixtures can be obtained from direct measurement of phase equilibrium data or by the use of equation of state and/or activity coefficient based on thermodynamic models. Direct measurement of precise experimental data is often difficult and expensive, while the second method, which includes a large number of equations of states and excess Gibbs free energy models, is tedious and involves a certain amount of empiricism to determine mixture constants, through fitting experimental data and using various arbitrary mixing rules, making it difficult to select the appropriate model for a particular case [9]. Thus due to the difficulties of experimental measurements and also their time-consuming and costly nature, it is desirable to develop predictive methods for estimating the phase behavior of these kinds of systems.

Artificial intelligence (AI) methods are advanced techniques, with extreme flexibility. ANN, as a branch of AI, is a flexible modeling method and has shown high performances in many cases. ANN is an empirical tool which can model any kind of data sets even in the cases where relations are complex [10]. Recently, ANN has found extensive application in the field of thermodynamics and transport properties such as the estimation of VLE, viscosity, density, vapor pressure, compressibility factor, and thermal conductivity [11–33]. This method provides nonlinear function mapping of a set of input variables into the corresponding network output. ANNs can be applied for accurate VLE determination of polar and nonpolar components [9, 34–51]. Basic theory and application to chemical problems of ANN with the back-propagation algorithm have been previously discussed in [48].

In this research, a comprehensive model based on multilayer feed forward back-propagation artificial neural network (FFBP-ANN) was developed to estimate VLE data for eight refrigerant mixtures containing CO_2. The refrigerants include difluoromethane (R32), propane (R290), 1,1-difluoroethane (R152a), hexafluoroethane (R116), decafluorobutane (R610), 2,2-dichloro-1,1,1-trifluoroethane (R123), 1-chloro-1,2,2,2-tetrafluoroethane (R124), and 1,1,1,2-tetrafluoroethane (R134a). The developed model was trained and evaluated by using the experimental data for eight binary refrigerant mixtures reported by [2–8] and pure component properties for eight refrigerants reported by [2–8, 52, 53]. A part of experimental data was used to train the networks, and the rest was used to evaluate the performance of the networks. Finally, for the model validation, the prediction of the ANN model (CO_2 mole fraction in the vapor phase) was compared with the thermodynamic model from different literatures [4, 6, 8] and also with the experimental data. Furthermore, the ability of the ANN model for the prediction of VLE data for binary mixture in azeotropic condition was examined.

2. Artificial Neural Network

Neural networks consist of arrays of simple active units linked by weighted connections. ANN consists of multiple layers of neurons arranged in such a way that each neuron in one layer is connected with each neuron in the next layer. The network used in this study is a multilayer feed forward neural network with a learning scheme of the back propagation (BP) of errors and the Levenberg-Marquardt algorithm for the adjustment of the connecting weights. Neurons are the fundamental processing element of an ANN, which are arranged in layers that make up the global architecture [48].

The main advantage of using ANNs to predict the VLE data lies in their ability to learn the relationship between the complex VLE data for different binary mixtures. The ANN input is the first layer in the network through which the information is supplied. The number of neurons in the input layer depends on the network input parameters. Hidden layers connect the input and output layers. Hidden layers enrich the network for learning the relation between input and output data. In theory, ANN with only one hidden layer and enough neurons in the hidden layer has the ability to learn any relation between the input and output data. Transfer function is the mathematic function that determines the relation between neuron output and the network. In other words, transfer function indicates the degree of nonlinearity in the network. Practically, in the feed forward BP-ANN model some limited functions are used as transfer functions [54]. Normally, the transfer functions of all neurons in the hidden layers are similar. Also, for all neurons in the output layer, the same transfer function is used. For the prediction of phenomena, logistic transfer function is the most conventional transfer function that is used in the hidden layers, because it is very easy to differentiate the sigmoid transfer function used in the BP algorithm [55, 56]. The sigmoid transfer function is as follows:

$$O_{Pj}\,(\text{net}) = \frac{1}{1 + e^{-\text{net}}}, \tag{1a}$$

$$\text{net} = \sum_{i=0}^{n-1} w_i x_i, \tag{1b}$$

where "n" in (1b) is the number of inputs to the neuron. "w_i" is the weight coefficient corresponding to the input "x_i" and "O_{Pj}" is the output corresponding to the "j" neuron. For completion of this section, we illustrate the learning BP algorithm.

2.1. ANN Training Algorithm. The back-propagation algorithm is one of the least mean square methods, which is normally used in engineering. In a multilayer perceptron, each neuron of a layer is linked to all neurons of the previous layer. Figure 1 shows a perceptron with a hidden layer.

Each layer output acts as the input to the next neurons. In order to train multilayer feed forward neural network, back-propagation law is used. In the first stage, all weights and biases are selected according to small random numbers. In the second stage, input vector $X_P = x_0, x_1, \ldots, x_{n-1}$ and the target exit $T_P = t_0, t_1, \ldots, t_{m-1}$ are given to the network, where the subscripts n and m are the numbers of input and output vectors, respectively. In the third stage, the following quantitative values are calculated and transferred to the subsequent layer until it eventually reaches the exit layer [57]

$$O_{Pj} = f\left[\sum_{i=0}^{n-1} w_i x_i\right]. \tag{2}$$

The fourth stage begins from the exit layer, during which the weight coefficients are corrected

$$w_{ij}\,(t+1) = w_{ij}\,(t) + \eta \delta_{Pj} O_{Pj}, \tag{3}$$

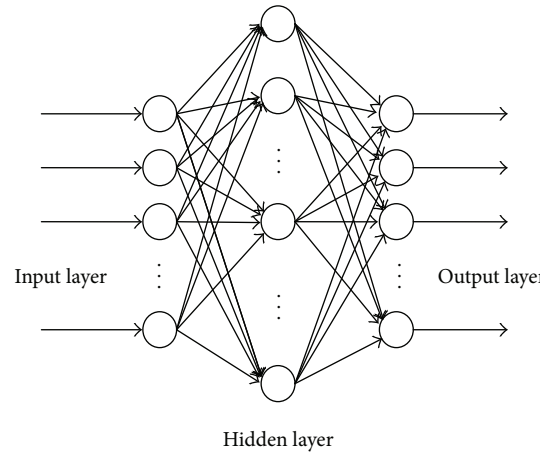

Figure 1: Perceptron structure with a hidden layer.

where "$w_{ij}(t)$" stands for the weight coefficients from node "i" to node "j" in time "t", "η" is the rate coefficient, "δ_{Pj}" refers to the corresponding error of input pattern "P" to the node "j", and "O_{Pj}" is the output corresponding to the "j" neuron. "δ_{Pj}" is calculated by the following equations for exit layer and hidden layer, respectively:

$$\begin{aligned} \delta_{Pj} &= O_{Pj}\left(1 - O_{Pj}\right)\left(t_{Pj} - O_{Pj}\right), \\ \delta_{Pj} &= O_{Pj}\left(1 - O_{Pj}\right)\sum_{k} \delta_{Pk} w_{jk}. \end{aligned} \tag{4}$$

Here, the $\sum$ acts for "k" nodes on the subsequent layer after the node "j" [57]. In the learning process, there are several parameters that have influence on the ANN training. These parameters are the number of iterations, number of hidden layers, and the number of hidden neurons. To find the best architecture of the model, the best set of the aforementioned parameters based on minimizing the network output error should be chosen.

3. Experimental Data

The first step in an ANN modeling is compiling the database to train the network and to evaluate network ability for generalization. In the present study, the experimental VLE data for eight binary mixtures reported by [2–8, 52, 53] have been used for training and validation of the ANN model. The range of the intensive state variables (temperature (T), pressure (P), and CO_2 mole fraction in the vapor (Y_1) and liquid (X_1) phases for each binary) and the number of data points (N) for the ANN training were listed in Table 1. Also, the pure component properties (normal boiling point (T_b), critical temperature (T_c), critical pressure (P_c), and acentric factor ω) of the eight refrigerants used in this work were collected from different literatures [2–8, 52, 53], and the collection was listed in Table 2.

Table 1: Experimental data range used for development of the ANN model.

Mixture	T (K)	P (MPa)	X_1	Y_1	N	Reference
R744 (1)-R32 (2)	283.12	1.106–4.508	0-1	0-1	56	[4]
	293.11	1.472–5.738	0-1	0-1		
	303.13	1.911–7.208	0-1	0-1		
	305.15	2.032–6.905	0–0.928	0–0.905		
	313.3	2.486–7.318	0–0.822	0–0.788		
	323.34	3.157–7.464	0–0.656	0–0.625		
	333.33	3.954–7.191	0–0.465	0–0.433		
	343.23	4.879–6.589	0–0.228	0–0.217		
R744 (1)-R152a (2)	258.44	0.144–2.294	0-1	0-1	67	[8]
	278.25	0.311–3.977	0-1	0-1		
	298.8	0.604–6.502	0-1	0-1		
	308.37	0.812–7.200	0–0.959	0–0.9355		
	323.3	1.185–7.648	0–0.8522	0–0.808		
	343.2	1.891–7.41	0–0.6710	0–0.5941		
R744 (1)-R290 (2)	253.15	0.244–1.964	0-1	0-1	124	[3]
	263.15	0.344–2.641	0-1	0-1		
	273.15	0.473–3.478	0-1	0-1		
	283.15	0.636–4.497	0-1	0-1		
	293.15	0.836–5.723	0-1	0-1		
	303.15	1.079–7.206	0-1	0-1		
	313.15	1.369–3.650	0–0.584	0–0.286		
	323.15	1.714–6.281	0–0.636	0–0.559		
R744 (1)-R116 (2)	253.29	2.043-1.051	0.0505–1	0.0284–1	75	[6]
	273.27	3.576-1.843	0.0385–1	0.0281–1		
	283.24	4.677-2.382	0.0685–1	0.0592–1		
	291.22	5.550-2.906	0.0244–1	0.0212–1		
	294.22	5.923–6.155	0.0145–0.1152	0.0132–0.1154		
	296.72	6.621-6.448	0.0096–0.0717	0.0090–0.0705		
R744 (1)-R610 (2)	263.15	0.1832–2.3997	0.5736–0.9830	0.0300–0.8900	83	[7]
	283	0.4589–3.9901	0.6253–0.9755	0.0636–0.9880		
	303.12	0.6544–6.6165	0.4800–0.9695	0.0593–0.9473		
	308.19	0.5021–6.8628	0.2418–0.9395	0.0218–0.9119		
	323.2	0.9625–6.7376	0.3719–0.8323	0.0565–0.7737		
	338.2	1.3940–6.3710	0.3448–0.7049	0.0713–0.6633		
	352.98	1.7097–5.5339	0.2492–0.5614	0.0638–0.5145		
R744 (1)-R123 (2)	313.15	0.873–7.189	0.8258–0.9788	0.1408–0.9209	18	[2]
	323.15	2.094–8.074	0.8975–0.9611	0.3073–0.9015		
	333.15	1.083–7.904	0.7352–0.9426	0.1219–0.8146		
R744 (1)-R124 (2)	313.15	0.594–7.256	0–0.9484	0–0.9096	22	[2]
	323.15	0.776–7.745	0–0.8878	0–0.8679		
	333.15	1.045–7.682	0–0.8231	0–0.7829		
R744 (1)-R134a (2)	252.95	0.131–1.685	0–0.983	0–0.867	29	[5]
	272.75	0.288–2.033	0–0.916	0–0.606		
	292.95	0.566–2.048	0–0.755	0–0.354		
	329.6	1.991–7.369	0.2412–0.7640	0.0821–0.7450		
	339.1	2.305–7.098	0.1781–0.6612	0.0666–0.6266		
	354	3.250–6.043	0.1733–0.4560	0.0826–0.3920		

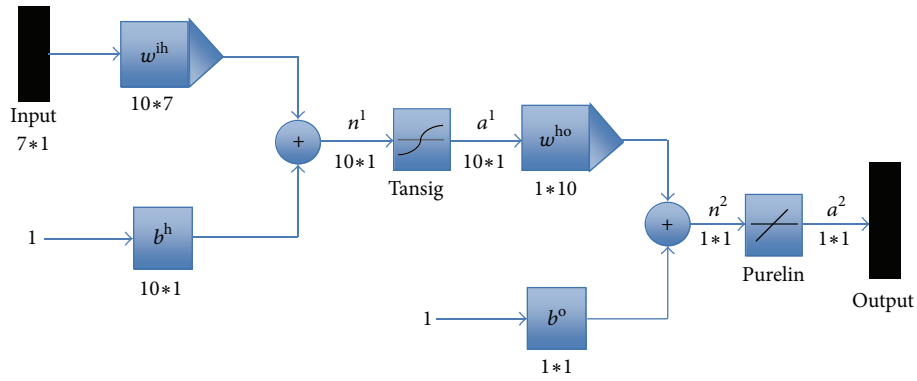

Figure 2: The feed forward back-propagation network used in the study.

Table 2: Pure component properties used in this work.

Component	T_b (K)	T_c (K)	P_c (MPa)	ω
R32	221.50	351.55	5.831	0.271
R290	231.07	369.82	4.242	0.149
R116	194.90	293.04	3.042	0.245
R152a	248.15	386.35	4.499	0.256
R610	271.20	385.84	2.289	0.374
R134a	246.93	374.25	4.064	0.326
R123	300.76	456.83	3.662	0.282
R124	261.04	395.43	3.624	0.2881

4. Development of the ANN Model

An ANN model was considered for the prediction of CO_2 mole fraction in the vapor phase. In order to describe the phase behavior of the eight R744 (1)-refrigerants (2) binaries by one ANN model a total of eight variables have been selected in this work: four intensive state variables (equilibrium temperature, equilibrium pressure, and equilibrium CO_2 mole fractions in the liquid and vapor phases) and four pure component properties of the refrigerant (normal boiling point, critical temperature, critical pressure, and acentric factor). The choice of the input and output variables was based on the phase rule, practical considerations (bubble or dew point computation), and the need to describe the eight binaries by only one ANN model. Therefore, the equilibrium temperature and pressure and the R744 mole fraction in the liquid phase together with the pure component properties of the refrigerant have been selected as input variables and the R744 mole fraction in the vapor phase as output variable.

As shown in Figure 2, a multilayer feed forward neural network structure with a hidden layer was used in this study. ANN modeling for the VLE of eight CO_2 (1)-refrigerant (2) binaries was carried out in MATLAB ver. 7.9.0 program. Initially, the program starts with the default FFBP-ANN type (*newff* MATLAB function), the *Levenberg-Marquardt BP* training algorithm (*trainlm* MATLAB training function), and one hidden layer. Once the topology is specified, the starting and ending number(s) of neurons in the hidden layer(s) have to be specified. The number of neurons in a hidden layer is then modified by adding neurons one at a time. The procedure begins with the logarithmic sigmoid activation function, then the hyperbolic tangent sigmoid activation function for the hidden layers, and the linear activation function for the output layer. The results of different runs of the program show that the bayesian regularization back propagation (BRBP), using Levenberg-Marquardt optimization models, train, more successfully than models using attenuated training. Table 3 shows the structure of the optimized ANN model. The weight matrices and bias vectors of the optimized ANN model were listed in Table 4, where w^{ih} is the input-hidden layer connection weight matrix (10 rows and 7 columns), w^{ho} is the hidden layer-output connection weight matrix (1 rows and 10 columns), b^h is the hidden neurons bias column vector (10 rows), and b^o is the output neurons bias column vector (1 row and 1 column).

5. Results and Discussion

Using the random selection method, 60% of all data were assigned to the training set, 20% of all data were assigned to the validation set, and the rest of the data were used as the test set. In the training phase, the number of neurons in the hidden layer was important for the network optimization. However, decision on the number of hidden layer neurons is difficult because it depends on the specific problem being solved using ANN. With too few neurons, the network may not be powerful enough for a given learning task. With a large number of neurons, the ANN may memorize the input training data very well so that the network tends to perform poorly on new test data and is called "overfitting". To prevent the overfitting issue, we should evaluate average absolute deviation (AAD) for train set, validation set, and test set and they must be in the same order of magnitude. Absolute deviation (AD) and AAD were calculated from the following relations:

$$\mathrm{AD} = \left|Y_1^{\mathrm{Exp}} - Y_1^{\mathrm{Calc}}\right|,$$
$$\mathrm{AAD} = \frac{1}{n}\sum_{i=1}^{n}\left|Y_{1,i}^{\mathrm{Exp}} - Y_{1,i}^{\mathrm{Calc}}\right|, \quad (5)$$

Table 3: Architecture of the optimized ANN.

Network type	Training algorithm	Input layer	Hidden layer		Output layer	
		No. of neurons	No. of neurons	Activation function	No. of neurons	Activation function
FFBP-ANN (*newff* MATLAB function)	BRBP using Levenberg-Marquardt optimization. (*trainbr* MATLAB function)	7	10	Logarithmic sigmoid (*logsig* MATLAB function)	1	Linear (*purelin* MATLAB function)

Table 4: Weights and Bias for the optimized ANN model.

Input-hidden layer connections								Hidden layer-output connections	
Weights							Bias	Weights	Bias
w_{j1}^{ih}	w_{j2}^{ih}	w_{j3}^{ih}	w_{j4}^{ih}	w_{j5}^{ih}	w_{j6}^{ih}	w_{j7}^{ih}	b_j^h	w_{1j}^{ho}	b^o
−0.6056	−0.9887	−0.7923	−0.6751	−0.4102	−1.5259	−3.0024	−0.2282	0.8706	
−0.134	0.1773	0.7049	−0.8568	0.9083	−0.0939	0.3924	0.2957	−2.7643	
0.1781	−0.0542	−0.1658	3.473	−4.3534	0.7277	−0.9445	−0.6808	4.6201	
−1.5473	−0.5041	−0.6426	−0.6926	2.273	0.3274	0.6674	2.1058	0.6233	
−0.1471	−1.69	−4.6153	−3.7246	4.0597	−1.133	0.4642	−7.8154	−4.8468	−4.6281
−0.5177	−0.8163	−0.7417	0.0359	−0.395	−1.0492	−2.267	−0.3021	−1.2227	
−0.3352	0.2159	0.3334	−3.1563	3.4222	−0.7444	0.625	0.2541	5.0439	
0.0599	−1.0839	2.4576	−2.211	1.0885	−0.0151	−0.8366	2.8284	−0.6923	
0.4007	−0.4818	1.0288	4.7919	−3.0998	1.0456	0.1107	1.1395	1.2612	
−0.1696	0.0643	1.0752	−0.4978	1.5478	0.1578	−0.0002	1.5111	1.7854	

where "n" is the number of data points and "Exp" and "Calc" superscripts stand for the experimental and calculated CO_2 mole fraction, respectively. In the training process, different hidden layers and neurons were tried, and finally the optimized ANN obtained for this study was a network with a hidden layer containing 10 neurons. In an optimized ANN, the AAD values for the train, validation, and test data sets are in the same order of magnitude. In this research, the AAD values for the train, validation, and test sets of data were obtained $2.851e-3$, $2.384e-3$, and $2.731e-3$, respectively, and the network performance (MSE) was achieved $1.3412e-5$. The ability of the model for the prediction of CO_2 mole fraction in the vapor phase is shown in Figure 3. As shown, good agreement for the prediction of ANN model and the experimental data are observed. So the developed ANN model can be used for the prediction of the new set of VLE data for the eight aforementioned binary mixtures.

To validate the ANN model prediction, the ability of the ANN model for the prediction of CO_2 mole fraction in the vapor phase of CO_2 (1) R152a (2) binary mixture at 308.3 K was investigated. Then the results were compared with Madani model [8]. The results were shown in Figure 4, and AD values for the ANN and Madani models were reported in Table 5. As shown, the maximum of the AD values for the ANN and Madani models were obtained 0.0124 and 0.0149, respectively. Also AAD for the ANN and Madani models were calculated 0.002969 and 0.002477, respectively. Thus AAD results for the ANN and Madani models are very close together.

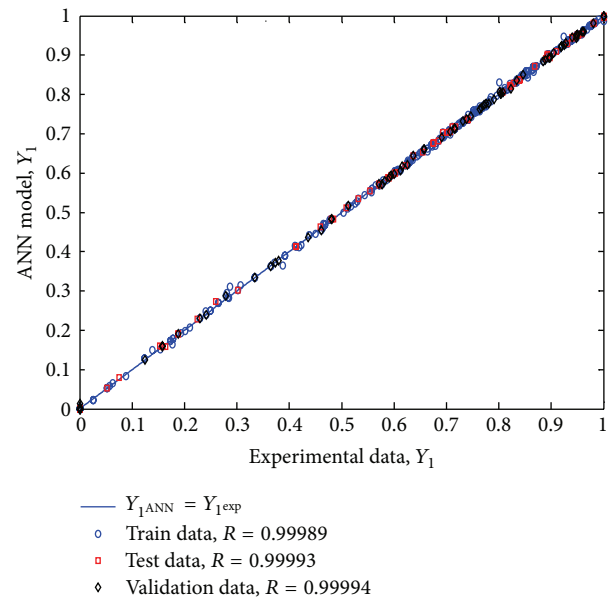

Figure 3: Comparison of the experimental and ANN model prediction for the mole fraction of CO_2 in eight binary mixtures.

In addition, Figure 5 compares the ANN results with thermodynamic model from the literature [6] and with the experimental results for R116-R744 binary mixture. The figure shows good agreement of the results with the experimental data. Also, Figure 5 shows that this comprehensive ANN

Table 5: Absolute deviation (AD) result for the ANN and Madani models for R744 (1)-R152a (2) mixture.

X_1	Y_1 experiment [8]	Y_1 Madani model [8]	Y_1 ANN model	AD Madani model [8]	AD ANN model
0	0	0	0	0	0
0.0722	0.3157	0.3306	0.3281	0.0149	0.0124
0.1419	0.493	0.4969	0.4898	0.0039	0.0032
0.2148	0.6097	0.6079	0.6041	0.0019	0.0056
0.295	0.6937	0.6897	0.6939	0.0041	0.0002
0.4194	0.7783	0.7756	0.7826	0.0028	0.0043
0.5197	0.8239	0.8239	0.8273	0	0.0034
0.6201	0.8621	0.8609	0.8621	0.0012	0
0.7176	0.8922	0.8921	0.8937	0.0001	0.0015
0.7994	0.9179	0.9174	0.9198	0.0006	0.0019
0.8755	0.9387	0.9391	0.9405	0.0004	0.0018
0.9152	0.9507	0.9525	0.9506	0.0018	0.0001
0.9355	0.9594	0.96	0.9552	0.0005	0.0042

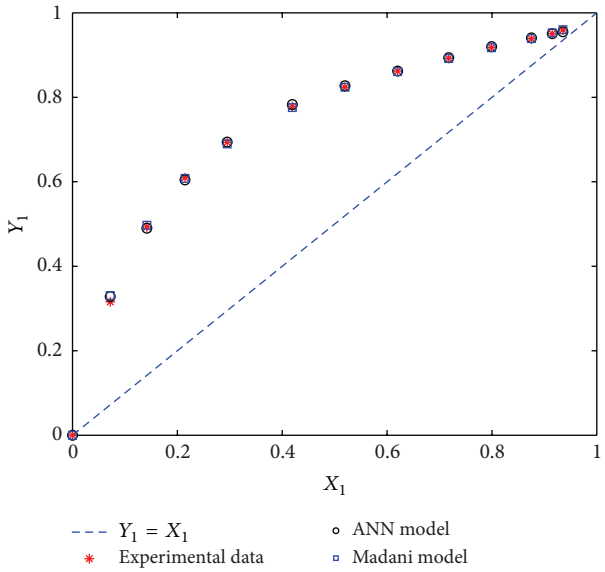

Figure 4: R744 mole fraction in vapor phase for binary system of R744 (1)-R152a (2) at 308.3 K (experimental data: [8], Madani Model: [8], and ANN model: this work).

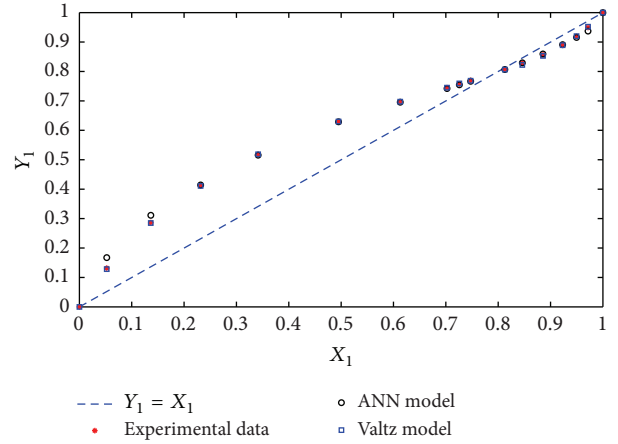

Figure 5: R744 mole fraction in vapor phase for binary system of R744 (1)-R116 (2) at 253.3 K (experimental data: [6], Valtz Model: [6], and ANN model: this work).

model can predict the azeotropic condition. Since the thermodynamic models are used for an especially binary mixture, while the developed ANN model is applicable for the eight aforementioned binary refrigerant mixtures, so this makes the ANN model an interesting predictive tool in respect to the thermodynamic models.

Figures 6, 7, 8, and 9 show the Y_1-X_1 curves for the binary mixtures of R610, R32, R134a, and R152a with CO_2. They include a comparison between experimental data and ANN results at different temperatures. As shown, the figures show excellent agreement between experimental data and the prediction of the ANN model. In addition, the AAD of the ANN model with the experimental data for the eight aforementioned binary mixtures at different temperatures were reported in Table 6. These results also indicate the predictability of the ANN model in the prediction of the CO_2 mole fraction in the vapor phase for the binary refrigerant mixtures.

6. Conclusions

In this work, a comprehensive FFBP-ANN model was developed for the prediction of VLE data. The model was constructed for eight conventional CO_2-containing binary refrigerant mixtures at different temperatures ranges. Binary refrigerants are CO_2-R32 mixture (283.15–343.23 K), CO_2-R290 (253.15–323.15 K), CO_2-R152a (258–343 K), CO_2-R116 (253.29–296.72 K), CO_2-R610 (263.15–352.98 K), CO_2-R123 (313.15–333.15 K), CO_2-R124 (313.15–333.15 K), and CO_2-R134a mixture (252.95–354 K). The optimized ANN model was obtained with a hidden layer and 10 neurons in the hidden layer. The input layer contains three intensive state

Table 6: AAD values for the ANN model in prediction of CO_2 mole fraction in different binary mixtures.

Mixture	T (K)	AAD
R744 (1)-R134a (2)	253	0.0031
	272	0.0032
	293	0.0063
	330	0.0037
	339	0.0031
	354	0.0025
R744 (1)-R124 (2)	313	0.0048
	323	0.0020
	333	0.0038
R744 (1)-R116 (2)	253	0.0066
	273	0.0043
	283	0.0049
	291	0.0023
	294	0.0007
	297	0.0005
R744 (1)-R290 (2)	253	0.0107
	263	0.0049
	273	0.0035
	283	0.0030
	293	0.0030
	303	0.0045
	313	0.0035
	323	0.0044
R744 (1)-R610 (2)	263	0.0163
	283	0.0025
	303	0.0025
	308	0.0018
	323	0.0035
	338	0.0036
	353	0.0024
R744 (1)-R32 (2)	283	0.0017
	293	0.0039
	303	0.0038
	305	0.0034
	313	0.0038
	323	0.0046
	333	0.0024
	343	0.0045
R744 (1)-R152a (2)	258	0.0021
	278	0.0040
	299	0.0047
	308	0.0030
	323	0.0035
	343	0.0025
R744 (1)-R123 (2)	313	0.0103
	323	0.0047
	333	0.0031

variables (equilibrium temperature, equilibrium pressure, and equilibrium CO_2 mole fraction in the liquid and vapour phases) and four pure component properties of the refrigerant (normal boiling point, critical temperature, critical pressure, and acentric factor). The output layer includes equilibrium CO_2 mole fraction in the vapor phase. In the ANN training procedure, the AAD for the sets of train, validation, and test data were obtained $2.851e-3$, $2.384e-3$, and $2.731e-3$, respectively, and the network performance (MSE) was achieved $1.3412e-5$. It was shown that excellent agreement between the model predictions and the experimental data was

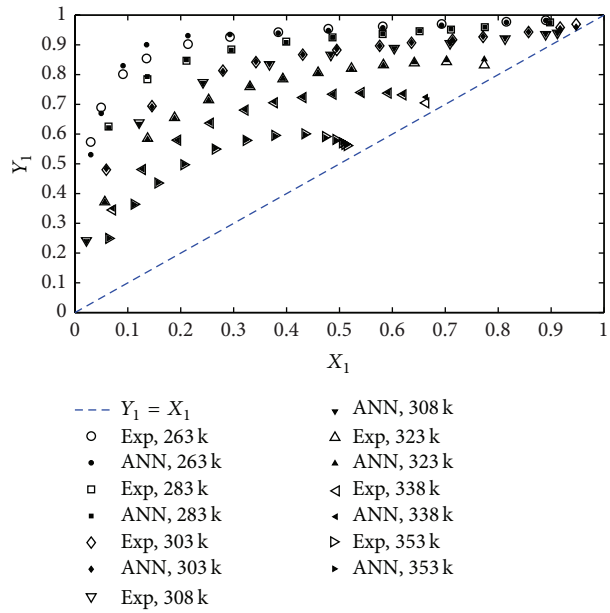

Figure 6: Y_1-X_1 curve for the R744 (1)-R610 (2) binary mixture at different temperatures (Exp: [7] and ANN: this work).

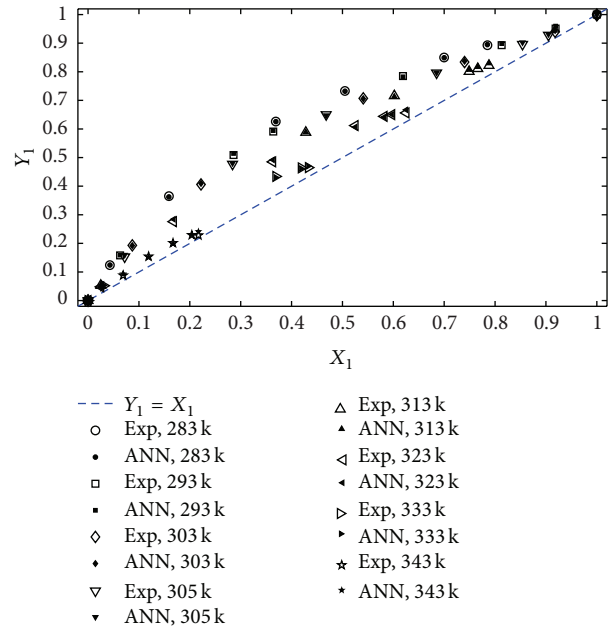

Figure 7: Y_1-X_1 curve for the R744 (1)-R32 (2) binary mixture at different temperatures (Exp: [4] and ANN: this work).

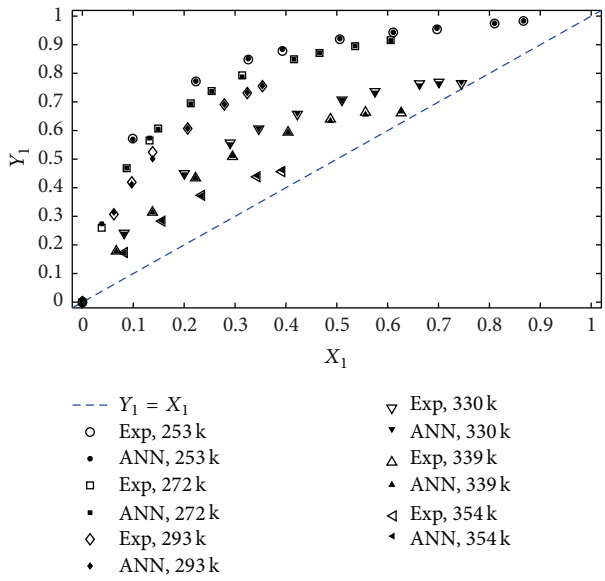

Figure 8: Y_1-X_1 curve for the R744 (1)-R134a (2) binary mixture at different temperatures (Exp: [5] and ANN: this work).

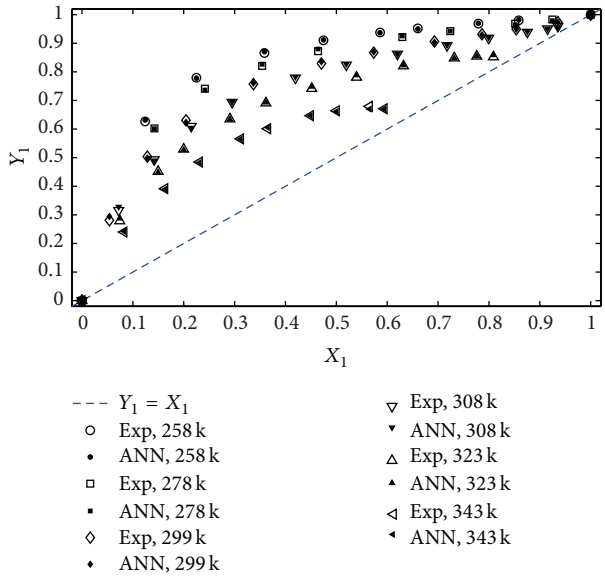

Figure 9: Y_1-X_1 curve for the R744 (1)-R152a (2) binary mixture at different temperatures (Exp: [8] and ANN: this work).

achieved. Also, the ability of the ANN model was examined in comparison with the different thermodynamic models for CO_2-R152a mixture at 308.3 K, CO_2-R32 at 343 K, and CO_2-R116 binary mixture at 253.3 K. The AAD results show that ANN model results are very close to the thermodynamic models. Also, ANN model can predict azeotropic condition for the CO_2-R116 binary mixture. Finally, the advantage of the ANN model is its applicability for the eight CO_2-containing binary mixtures, while the thermodynamic models are used for an especially binary mixture.

References

[1] J. S. Lim, J. M. Jin, and K.-P. Yoo, "VLE measurement for binary systems of CO_2 + 1,1,1,2-tetrafluoroethane (HFC-134a) at high pressures," *The Journal of Supercritical Fluids*, vol. 44, no. 3, pp. 279–283, 2008.

[2] K. Jeong, J. Im, G. Lee, Y.-J. Lee, and H. Kim, "Vapor-liquid equilibria of the carbon dioxide (CO_2) + 2,2-dichloro-1,1,1-trifluoroethane (R123) system and carbon dioxide (CO_2) + 1-chloro-1,2,2,2-tetrafluoroethane (R124) system," *Fluid Phase Equilibria*, vol. 251, no. 1, pp. 63–67, 2007.

[3] J. H. Kim and M. S. Kim, "Vapor-liquid equilibria for the carbon dioxide + propane system over a temperature range from 253.15 to 323.15 K," *Fluid Phase Equilibria*, vol. 238, no. 1, pp. 13–19, 2005.

[4] F. Rivollet, A. Chapoy, C. Coquelet, and D. Richon, "Vapor-liquid equilibrium data for the carbon dioxide (CO_2) + difluoromethane (R32) system at temperatures from 283.12 to 343.25 K and pressures up to 7.46 MPa," *Fluid Phase Equilibria*, vol. 218, no. 1, pp. 95–101, 2004.

[5] G. Silva-Oliver and L. A. Galicia-Luna, "Vapor-liquid equilibria for carbon dioxide + 1,1,1,2-tetrafluoroethane (R-134a) systems at temperatures from 329 to 354 K and pressures upto 7.37 MPa," *Fluid Phase Equilibria*, vol. 199, no. 1-2, pp. 213–222, 2002.

[6] A. Valtz, C. Coquelet, and D. Richon, "Vapor-liquid equilibrium data for the hexafluoroethane + carbon dioxide system at temperatures from 253 to 297 K and pressures up to 6.5 MPa," *Fluid Phase Equilibria*, vol. 258, no. 2, pp. 179–185, 2007.

[7] A. Valtz, X. Courtial, E. Johansson, C. Coquelet, and D. Ramjugernath, "Isothermal vapor-liquid equilibrium data for the carbon dioxide (R744) + decafluorobutane (R610) system at temperatures from 263 to 353K," *Fluid Phase Equilibria*, vol. 304, no. 1-2, pp. 44–51, 2011.

[8] H. Madani, A. Valtz, C. Coquelet, A. H. Meniai, and D. Richon, "(Vapor + liquid) equilibrium data for (carbon dioxide + 1,1-difluoroethane) system at temperatures from (258 to 343) K and pressures up to about 8 MPa," *The Journal of Chemical Thermodynamics*, vol. 40, no. 10, pp. 1490–1494, 2008.

[9] C. Si-Moussa, S. Hanini, R. Derriche, M. Bouhedda, and A. Bouzidi, "Prediction of high-pressure vapor liquid equilibrium of six binary systems, carbon dioxide with six esters, using an artificial neural network model," *Brazilian Journal of Chemical Engineering*, vol. 25, no. 1, pp. 183–199, 2008.

[10] M. N. Safamirzaei, H. Modarress, and M. Mohsen-Nia, "Modeling the hydrogen solubility in methanol, ethanol, 1-propanol and 1-butanol," *Fluid Phase Equilibria*, vol. 289, no. 1, pp. 32–39, 2010.

[11] H. Ghanadzadeh, M. Ganji, and S. Fallahi, "Mathematical model of liquid-liquid equilibrium for a ternary system using the GMDH-type neural network and genetic algorithm," *Applied Mathematical Modelling*, vol. 36, no. 9, pp. 409–4105, 2012.

[12] V. H. Alvarez and M. D. A. Saldaña, "Thermodynamic prediction of vapor-liquid equilibrium of supercritical CO_2 or CHF_3 + ionic liquids," *The Journal of Supercritical Fluids*, vol. 66, pp. 29–35, 2012.

[13] F. Gharagheizi, A. Eslamimanesh, P. Ilani-Kashkouli, A. H. Mohammadi, and D. Richon, "Determination of vapor pressure of chemical compounds: a group contribution model for an extremely large database," *Industrial & Engineering Chemistry Research*, vol. 51, pp. 7119–7125, 2012.

[14] A. Z. Hezave, M. Lashkarbolooki, and S. Raeissi, "Correlating bubble points of ternary systems involving nine solvents and two ionic liquids using artificial neural network," *Fluid Phase Equilibria*, vol. 352, pp. 34–41, 2013.

[15] M. Lashkarblooki, A. Z. Hezave, A. M. Al-Ajmi, and S. Ayatollahi, "Viscosity prediction of ternary mixtures containing ILs using multi-layer perceptron artificial neural network," *Fluid Phase Equilibria*, vol. 326, pp. 15–20, 2012.

[16] M. Lashkarbolooki, A. Z. Hezave, and S. Ayatollahi, "Artificial neural network as an applicable tool to predict the binary heat capacity of mixtures containing ionic liquids," *Fluid Phase Equilibria*, vol. 324, pp. 102–107, 2012.

[17] M. Safamirzaei and H. Modarress, "Correlating and predicting low pressure solubility of gases in [bmim][BF_4] by neural network molecular modeling," *Thermochimica Acta*, vol. 545, pp. 125–130, 2012.

[18] A. Şencan Şahin and H. Yazıcı, "Thermodynamic evaluation of the Afyon geothermal district heating system by using neural network and neuro-fuzzy," *Journal of Volcanology and Geothermal Research*, vol. 233-234, pp. 65–71, 2012.

[19] Y. Sun, G. Bian, W. Tao, C. Zhai, M. Zhong, and Z. Qiao, "Thermodynamic optimization and calculation of the YCl_3-ACl (A=Li, Na, K, Rb, Cs) phase diagrams," *Calphad*, vol. 39, pp. 1–10, 2012.

[20] X. Xiao, G. Q. Liu, B. F. Hu et al., "A comparative study on Arrhenius-type constitutive equations and artificial neural network model to predict high-temperature deformation behaviour in 12Cr3WV steel," *Computational Materials Science*, vol. 62, pp. 227–234, 2012.

[21] K. M. Yerramsetty, B. J. Neely, and K. M. Gasem, "A nonlinear structure-property model for octanol-water partition coefficient," *Fluid Phase Equilibria*, vol. 332, pp. 85–93, 2012.

[22] F. Yousefi and H. Karimi, "P-V-T properties of polymer melts based on equation of state and neural network," *European Polymer Journal*, vol. 48, pp. 1135–1143, 2012.

[23] F. Yousefi, H. Karimi, and M. M. Papari, "Modeling viscosity of nanofluids using diffusional neural networks," *Journal of Molecular Liquids*, vol. 175, pp. 85–90, 2012.

[24] M. Safamirzaei and H. Modarress, "Application of neural network molecular modeling for correlating and predicting Henry's law constants of gases in [bmim][PF_6] at low pressures," *Fluid Phase Equilibria*, vol. 332, pp. 165–172, 2012.

[25] K. Shahbaz, S. Baroutian, F. S. Mjalli, M. A. Hashim, and I. M. Alnashef, "Densities of ammonium and phosphonium based deep eutectic solvents: prediction using artificial intelligence and group contribution techniques," *Thermochimica Acta*, vol. 527, pp. 59–66, 2012.

[26] F. Gharagheizi, P. Ilani-Kashkouli, N. Farahani, and A. H. Mohammadi, "Gene expression programming strategy for estimation of flash point temperature of non-electrolyte organic compounds," *Fluid Phase Equilibria*, vol. 329, pp. 71–77, 2012.

[27] I. P. Koronaki, E. Rogdakis, and T. Kakatsiou, "Thermodynamic analysis of an open cycle solid desiccant cooling system using artificial neural network," *Energy Conversion and Management*, vol. 60, pp. 152–160, 2012.

[28] T. Hatami, M. Rahimi, H. Daraei, E. Heidaryan, and A. A. Alsairafi, "PRSV equation of state parameter modeling through artificial neural network and adaptive network-based fuzzy inference system," *Korean Journal of Chemical Engineering*, vol. 29, no. 5, pp. 657–667, 2012.

[29] M. Saber, "Comparative analysis of hydrate formation pressure applying cubic Equations of State (EoS), Artificial Neural Network (ANN) and Adaptive Neuro-Fuzzy Inference System (ANFIS)," *International Journal of Thermodynamics*, vol. 15, pp. 91–101, 2012.

[30] F. Gharagheizi, A. Eslamimanesh, P. Ilani-Kashkouli, A. H. Mohammadi, and D. Richon, "QSPR molecular approach for representation/prediction of very large vapor pressure dataset," *Chemical Engineering Science*, vol. 76, pp. 99–107, 2012.

[31] F. Hajabdollahi, Z. Hajabdollahi, and H. Hajabdollahi, "Soft computing based multi-objective optimization of steam cycle power plant using NSGA-II and ANN," *Applied Soft Computing*, vol. 12, no. 11, pp. 3648–3655, 2012.

[32] H. Karimi and F. Yousefi, "Application of artificial neural network-genetic algorithm (ANN-GA) to correlation of density in nanofluids," *Fluid Phase Equilibria*, vol. 336, pp. 79–83, 2012.

[33] S. Zendehboudi, M. A. Ahmadi, L. James, and I. Chatzis, "Prediction of condensate-to-gas ratio for retrograde gas condensate reservoirs using artificial neural network with particle swarm optimization," *Energy & Fuels*, vol. 26, pp. 3432–3447, 2012.

[34] S. Urata, A. Takada, J. Murata, T. Hiaki, and A. Sekiya, "Prediction of vapor-liquid equilibrium for binary systems containing HFEs by using artificial neural network," *Fluid Phase Equilibria*, vol. 199, no. 1-2, pp. 63–78, 2002.

[35] R. Sharma, D. Singhal, R. Ghosh, and A. Dwivedi, "Potential applications of artificial neural networks to thermodynamics: vapor—liquid equilibrium predictions," *Computers & Chemical Engineering*, vol. 23, no. 3, pp. 385–390, 1999.

[36] S. Mohanty, "Estimation of vapour liquid equilibria of binary systems, carbon dioxide-ethyl caproate, ethyl caprylate and ethyl caprate using artificial neural networks," *Fluid Phase Equilibria*, vol. 235, no. 1, pp. 92–98, 2005.

[37] C. A. Faúndez, F. A. Quiero, and J. O. Valderrama, "Phase equilibrium modeling in ethanol + congener mixtures using an artificial neural network," *Fluid Phase Equilibria*, vol. 292, no. 1-2, pp. 29–35, 2010.

[38] M. C. Iliuta, I. Iliuta, and F. Larachi, "Vapour-liquid equilibrium data analysis for mixed solvent-electrolyte systems using neural network models," *Chemical Engineering Science*, vol. 55, no. 15, pp. 2813–2825, 2000.

[39] S. Mohanty, "Estimation of vapour liquid equilibria for the system carbon dioxide-difluoromethane using artificial neural networks," *International Journal of Refrigeration*, vol. 29, no. 2, pp. 243–249, 2006.

[40] A. Mun, A. K. Mutlag, and M. S. Hameed, "Vapor-liquid equilibrium prediction by PE and ANN for the extraction of unsaturated fatty acid esters by supercritical CO_2," *Network*, vol. 6, no. 9, pp. 122–134, 2011.

[41] A. Ghaemi, S. Shahhoseini, M. Ghannadi, and M. Farrokhi, "Prediction of vapor-liquid equilibrium for aqueous solutions of electrolytes using artificial neural networks," *Journal of Applied Sciences*, vol. 8, no. 4, pp. 615–621, 2008.

[42] M. Bilgin, "Isobaric vapour—liquid equilibrium calculations of binary systems using a neural network," *Journal of the Serbian Chemical Society*, vol. 69, no. 8-9, pp. 669–674, 2004.

[43] H. Yamamoto and K. Tochigi, "Prediction of vapor—liquid equilibria using reconstruction-learning neural network method," *Fluid Phase Equilibria*, vol. 257, no. 2, pp. 169–172, 2007.

[44] B. Zarenezhad and A. Aminian, "Predicting the vapor-liquid equilibrium of carbon dioxide + alkanol systems by using an artificial neural network," *Korean Journal of Chemical Engineering*, vol. 28, no. 5, pp. 1286–1292, 2011.

[45] R. Abedini, I. Zanganeh, and M. Mohagheghian, "Simulation and estimation of vapor-liquid equilibrium for asymmetric binary systems (CO_2-Alcohols) using artificial neural network," *Journal of Phase Equilibria and Diffusion*, vol. 32, no. 2, pp. 105–114, 2011.

[46] S. Ganguly, "Prediction of VLE data using radial basis function network," *Computers & Chemical Engineering*, vol. 27, no. 10, pp. 1445–1454, 2003.

[47] C. A. Faúndez, F. A. Quiero, and J. O. Valderrama, "Correlation and prediction of VLE of water + congener mixtures found in alcoholic beverages using an artificial neural network," *Chemical Engineering Communications*, vol. 198, no. 1, pp. 102–119, 2010.

[48] H. Karimi and F. Yousefi, "Correlation of vapour liquid equilibria of binary mixtures using artificial neural networks," *Chinese Journal of Chemical Engineering*, vol. 15, no. 5, pp. 765–771, 2007.

[49] H. Ghanadzadeh and H. Ahmadifar, "Estimation of (vapour + liquid) equilibrium of binary systems (*tert*-butanol + 2-ethyl-1-hexanol) and (*n*-butanol + 2-ethyl-1-hexanol) using an artificial neural network," *The Journal of Chemical Thermodynamics*, vol. 40, no. 7, pp. 1152–1156, 2008.

[50] T. Hiaki, M. Nanao, S. Urata, and J. Murata, "Vapor—liquid equilibria for 1,1,2,3,3,3-hexafluoropropyl, 2,2,2-trifluoroethyl ether with several organic solvents," *Fluid Phase Equilibria*, vol. 194–197, pp. 969–979, 2002.

[51] S. Ketabchi, H. Ghanadzadeh, A. Ghanadzadeh, S. Fallahi, and M. Ganji, "Estimation of VLE of binary systems (*tert*-butanol + 2-ethyl-1-hexanol) and (*n*-butanol + 2-ethyl-1-hexanol) using GMDH-type neural network," *The Journal of Chemical Thermodynamics*, vol. 42, no. 11, pp. 1352–1355, 2010.

[52] AspenONE, Aspen Hysys 2006 Software.

[53] M. O. McLinden, "Thermodynamic properties of CFC alternatives: a survey of the available data," *International Journal of Refrigeration*, vol. 13, no. 3, pp. 149–162, 1990.

[54] G. Zhang, B. E. Patuwo, and M. Y. Hu, "Forecasting with artificial neural networks: the state of the art," *International Journal of Forecasting*, vol. 14, no. 1, pp. 35–62, 1998.

[55] A. Malallah and I. S. Nashawi, "Estimating the fracture gradient coefficient using neural networks for a field in the Middle East," *Journal of Petroleum Science and Engineering*, vol. 49, no. 3-4, pp. 193–211, 2005.

[56] M. Chakraborty, C. Bhattacharya, and S. Dutta, "Studies on the applicability of Artificial Neural Network (ANN) in emulsion liquid membranes," *Journal of Membrane Science*, vol. 220, no. 1-2, pp. 155–164, 2003.

[57] R. Beale and T. Jackson, *Neural Computing: An Introduction*, Institude of Physics, London, UK, 1998.